Article

Conformational Preferences of an Amyloidogenic Peptide: IR Spectroscopy of Ac-VQIVYK-NHMe

Timothy D. Vaden, Sally A. N. Gowers, Tjalling S. J. A. de Boer, Jeffrey D. Steill, Jos Oomens, and Lavina C. Snoek

J. Am. Chem. Soc., **2008**, 130 (44), 14640-14650 • DOI: 10.1021/ja804213s • Publication Date (Web): 10 October 2008

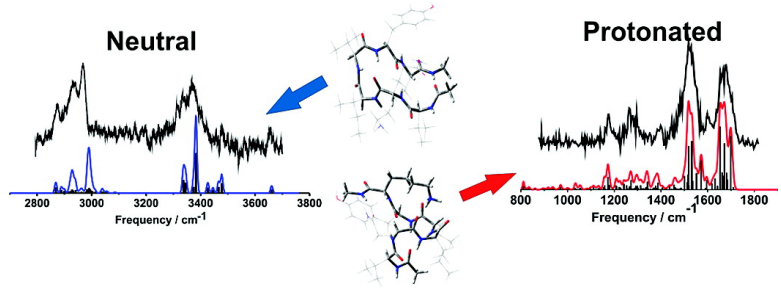

More About This Article

Additional resources and features associated with this article are available within the HTML version:

- Supporting Information
- Access to high resolution figures
- Links to articles and content related to this article
- Copyright permission to reproduce figures and/or text from this article

View the Full Text HTML

J|A|C|S
ARTICLES

Published on Web 10/10/2008

Conformational Preferences of an Amyloidogenic Peptide: IR Spectroscopy of Ac-VQIVYK-NHMe

Timothy D. Vaden,[†,*] Sally A. N. Gowers,[†] Tjalling S. J. A. de Boer,[†] Jeffrey D. Steill,[‡] Jos Oomens,[‡] and Lavina C. Snoek[†]

Department of Chemistry, Physical and Theoretical Chemistry Laboratory, University of Oxford, South Parks Road, Oxford OX1 3QZ, U.K., and FOM Institute for Plasma Physics Rijnhuizen, Edisonbaan 14, 3439 MN Nieuwegein, The Netherlands

Received June 4, 2008; E-mail: timothy.vaden@chem.ox.ac.uk; lavina.snoek@chem.ox.ac.uk

Abstract: The ^{306}VQIVYK^{311} sequence in the tau peptide is essential for the formation of intracellular amyloid fibrils related to Alzheimer's disease, where it forms interdigitating cross-β-structures. The inherent conformational preferences of the capped hexapeptide Ac-VQIVYK-NHMe were characterized in the gas phase. IR/UV double-resonance spectroscopy of the peptide isolated in a cold molecular beam was used to probe the conformation of the neutral peptide. The influence of protonation at the lysine side chain was investigated at 298 K by characterizing the protonated peptide ion, Ac-VQIVYK(H^+)-NHMe, with IRMPD spectroscopy in the fingerprint and amide I/II band region in an FTICR mass spectrometer. The conformations for both neutral and protonated peptides were predicted by an extensive conformational search procedure followed by cluster analysis and then DFT calculations. Comparison of the experimental and computed IR spectra, with consideration of the relative energies, was used to assign the dominant conformations observed. The neutral peptide adopts a β-hairpin-like conformation with two loosely extended peptide chains, demonstrating the preference of the sequence for extended β-strand-like structures. In the protonated peptide, the lysine NH_3^+ disrupts this extended conformation by binding to the backbone and induces a transition to a random-coil-like structure.

Introduction

Amyloidoses, such as Alzheimer's disease (AD) and type II diabetes, are a class of "protein misfolding" diseases characterized by the formation of insoluble amyloid fibrils from normal, "physiologically healthy" proteins. Much of the current research on these diseases focuses on the causes and nature of amyloid fibril formation[1−3] as well as the physiological implications of amyloid.[4,5] With respect to the former research area, it is of clear importance to understand the structures of amyloid fibrils and the factors influencing their formation at a molecular level. To this end, amyloid fibril structures have been characterized using solid-state NMR[6] and X-ray crystallography.[7] Amyloid fibrils have high β-sheet content;[7] the well-characterized β-amyloid (Aβ) and tau-peptide fibrils, related to AD, are composed of β-sheet-structured monomers aggregated via noncovalent interactions between β-strands.[7,8] Such β-sheet motifs are predicted to be thermodynamically favorable relative to native conformations, which may explain why they can be formed, even in vitro.[3] In particular, a molecular-level understanding of amyloid structures will shed light on the reasons they *are* formed (different from why they *can* be formed).

In AD, Aβ proteins form extracellular amyloid fibrils, while the tau peptide forms intracellular amyloid in the form of paired helical filaments (PHF) and single filaments (SF).[7−9] In both the PHF and SF amyloid, the tau peptides aggregate via cross-β hydrogen bonding, where two monomer β-sheet structures adhere together.[7,8] The most important amino acid sequence in the tau peptide is ^{306}VQIVYK^{311}, as this sequence has been shown to be necessary for amyloid formation[10−12] through the cross-β interactions.[13] Indeed, the capped hexapeptide Ac-VQIVYK-NH_2 by itself forms insoluble β-sheet aggregates spontaneously in aqueous solution.[11] Thus, the ^{306}VQIVYK^{311} sequence is a representative building block of a "steric zipper" motif common to many different amyloid fibrils, where the side

† University of Oxford.
‡ FOM Institute for Plasma Physics.

(1) Chiti, F.; Dobson, C. M. *Annu. Rev. Biochem.* **2006**, *75*, 333–366.
(2) Eisenberg, D.; Nelson, R.; Sawaya, M. R.; Balbirnie, M.; Sambashivan, S.; Ivanova, M. I.; Madsen, A. Ø.; Riekel, C. *Acc. Chem. Res.* **2006**, *39*, 568–575.
(3) Perczel, A.; Hudaky, P.; Palfi, V. K. *J. Am. Chem. Soc.* **2007**, *129*, 14959–14965.
(4) Marchesi, V. T. *Proc. Natl. Acad. Sci. U.S.A.* **2005**, *102*, 9093–9098.
(5) Teplow, D. B.; Lazo, N. L.; Bitan, G.; Bernstein, S.; Wyttenbach, T.; Bowers, M. T.; Baumketner, A.; Shea, J.-E.; Urbanc, B.; Cruz, L.; Borreguero, J.; Stanley, H. E. *Acc. Chem. Res.* **2006**, *39*, 635–645.
(6) Tycko, R. *Q. Rev. Biophys.* **2006**, *39*, 1–55.
(7) Makin, O. S.; Serpell, L. C. *FEBS J.* **2005**, *272*, 5950–5961.
(8) Berriman, J.; Serpell, L. C.; Oberg, K. A.; Fink, A. L.; Goedert, M.; Crowther, R. A. *Proc. Natl. Acad. Sci. U.S.A.* **2003**, *100*, 9034–9038.
(9) Crowther, R. A.; Goedert, M. *J. Struct. Biol.* **2000**, *130*, 271–279.
(10) Perez, M.; Santa-Maria, I.; Tortosa, E.; Cuadros, R.; del Valle, M.; Hernandez, F.; Moreno, F. J.; Avila, J. *J. Neurochem.* **2007**, *103*, 1447–1460.
(11) Quijano, F. A. R.; Morrow, D.; Wise, B. M.; Brancia, F. L.; Goux, W. J. *Biochemistry* **2006**, *45*, 4638–4652.
(12) von Bergen, M.; Friedhoff, P.; Biernat, J.; Heberle, J.; Mandelkow, E.-M.; Mandelkow, E. *Proc. Natl. Acad. Sci. U.S.A.* **2000**, *97*, 5129–5134.
(13) Sawaya, M. R.; Sambashivan, S.; Nelson, R.; Ivanova, M. I.; Sievers, S. A.; Apostol, M. I.; Thompson, M. J.; Balbirnie, M.; Wiltzius, J. J. W.; McFarlane, H. T.; Madsen, A. Ø.; Riekel, C.; Eisenberg, D. *Nature* **2007**, *447*, 453–457.

 10.1021/ja804213s CCC: $40.75

chain of the β-strand of one unit interdigitates with the same sequence on another monomer to support amyloid formation.[13]

Understanding the preferred conformational landscape of the isolated ^{306}VQIVYK^{311} sequence in the absence of the biological medium may yield valuable insight into the amyloid formation process, regarding the inherent stability of the β-sheet and steric zipper structures and the intramolecular forces that influence these structures. Such details about the peptide structure may be highlighted by comparing and contrasting the conformation(s) observed in the gas-phase peptide with the β-sheet structure in the amyloid fibril. Indeed, a recent suggestion is to target amyloidogenic sequences like the tau ^{306}VQIVYK^{311} to design more effective anti-amyloid drugs,[14] further underscoring the need to understand the peptide conformational landscape. Studies of neutral gas-phase single peptides (in a ~10 K molecular beam) by Mons and co-workers,[15−17] de Vries and co-workers,[18,19] and Kleinermanns and co-workers[20] (among others) and model β-sheet dimers by Gerhards and co-workers[21,22] have shown that IR/UV double-resonance spectroscopy combined with DFT and ab initio calculations is a valuable and sensitive tool for characterizing the energetically favorable conformations of small and moderately sized peptides, and they have elucidated important relationships between gas-phase peptides and "real world" proteins. By identifying traditional secondary-structure *motifs* such as helices,[16,23] β- and γ-turns,[16,24] and (relevant to the current work) β-sheets[21,22] in gas-phase peptides, it has become possible to draw relevant comparisons and contrasts with X-ray crystallography and NMR data.

With the specific VQIVYK sequence, it is also of interest to understand the effect of protonation at the lysine side chain NH_2 on the peptide conformation. This protonation introduces a positive charge to the peptide, and it is known that noncovalent inter- and intramolecular interactions involving ionic forces can be very strong (on the order of 50−100 kJ/mol, or even more) and significantly influence peptide conformational landscapes, both in the gas phase[25] and in "real" proteins. Protonated peptide conformations have been investigated by many groups, including our groups,[25−28] by combining mass spectrometry with infrared multiple photon dissociation (IRMPD) spectroscopy.[27] Vibrational band positions observed in IRMPD spectra are in principle slightly red-shifted relative to single-photon IR spectra due to vibrational anharmonicity, and relative IRMPD intensities do not always follow single-photon IR intensities.[27] Nevertheless, IRMPD spectroscopy has been applied successfully for the study

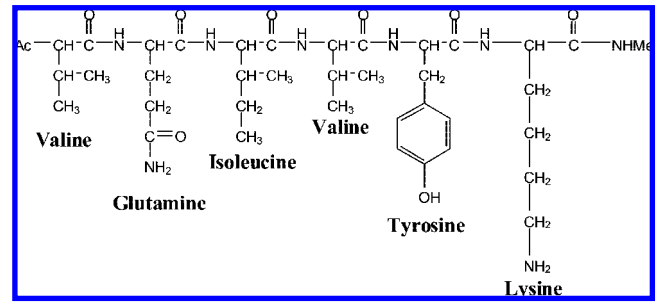

Figure 1. Structure of the Ac-VQIVYK-NHMe peptide characterized in this work.

of protonated amino acids and peptides,[29−31] because the anharmonicity shifts are often small (~1−2%)[32] relative to the instrument resolution, and relative IRMPD intensities are usually sufficiently similar to single-photon intensities to enable spectroscopic assignment.

Recently, Polfer et al. have demonstrated the characterization of a relatively large protonated peptide conformation (H^+-enkephalin, five amino acids) using electrospray ionization fourier transform ion cyclotron resonance (ESI-FTICR) mass spectrometry combined with IRMPD spectroscopy of the amide I/II bands using a free electron laser (FEL).[28] In this technique, the peptide ions are at room temperature, in contrast to the experiments noted for neutral molecular beam investigations (~15−20 K, vide infra). Because of the elevated temperature, this is a significantly different type of experiment. The observed conformations are influenced by entropy, as well as energy, although it should be noted that the free-energy-favored conformation at 298 K is often not too different from that at 0 K. More importantly, however, the very nature of the conformations is different: while peptides at 0 K are frozen into one or a few distinct structures, at 298 K peptides are better described in terms of an average conformation, with a (relatively) rigid backbone and moderate- or large-amplitude side-chain motions.[33] Nonetheless, the general information obtained regarding the conformational landscape is relevant to understanding the differences between the neutral and protonated Ac-VQIVYK-NHMe peptide.

In this work, we characterize the inherent gas-phase conformation of the ^{306}VQIVYK^{311} sequence by studying it as a capped hexapeptide fragment, Ac-VQIVYK-NHMe, shown in Figure 1. This investigation reveals the preferred conformations of the peptide molecule in the absence of the biological medium, where the side chains may be solvated by water molecules or otherwise interact with other peptide molecules in the full tau protein (either in the native state or amyloid fibril). Extensive molecular-mechanics-based conformational searches, followed

(14) Esteras-Chopo, A.; Pastor, M. T.; Serrano, L.; Lopez de la Paz, M. *J. Mol. Biol.* **2008**, *377*, 1372–1381.
(15) Brenner, V.; Piuzzi, F.; Dimicoli, I.; Tardivel, B.; Mons, M. *J. Phys. Chem. A* **2007**, *111*, 7347–7354.
(16) Chin, W.; Piuzzi, F.; Dimicoli, I.; Mons, M. *Phys. Chem. Chem. Phys.* **2006**, *8*, 1033–1048.
(17) Gloaguen, E.; Pagliarulo, F.; Brenner, V.; Chin, W.; Piuzzi, F.; Tardivel, B.; Mons, M. *Phys. Chem. Chem. Phys.* **2007**, *9*, 4491–4497.
(18) Abo-Riziq, A.; Crews, B. O.; Callahan, M. P.; Grace, L.; de Vries, M. S. *Angew. Chem., Int. Ed.* **2006**, *45*, 5166–5169.
(19) De Vries, M. S.; Hobza, P. *Annu. Rev. Phys. Chem.* **2007**, *58*, 585–612.
(20) Haber, T.; Seefeld, K.; Kleinermanns, K. *J. Phys. Chem. A* **2007**, *111*, 3038–3046.
(21) Fricke, H.; Funk, A.; Schrader, T.; Gerhards, M. *J. Am. Chem. Soc.* **2008**, *130*, 4692–4698.
(22) Gerhards, M.; Unterberg, C.; Gerlach, A. *Phys. Chem. Chem. Phys.* **2002**, *4*, 5563–5565.
(23) Chin, W.; Piuzzi, F.; Dognon, J.-P.; Dimicoli, I.; Tardivel, B.; Mons, M. *J. Am. Chem. Soc.* **2005**, *127*, 11900–11901.
(24) Compagnon, I.; Oomens, J.; Bakker, J.; Meijer, G.; Von Helden, G. *Phys. Chem. Chem. Phys.* **2005**, *7*, 13–15.
(25) Vaden, T. D.; de Boer, T. S. J. A.; Simons, J. P.; Snoek, L. C. *Phys. Chem. Chem. Phys.* **2008**, *10*, 1443–1447.
(26) Vaden, T. D.; De Boer, T. S. J. A.; Simons, J. P.; Snoek, L. C.; Suhai, S.; Paizs, B. *J. Phys. Chem. A* **2008**, *112*, 4608–4616.
(27) Oomens, J.; Satarkov, B. G.; Meijer, G.; von Helden, G. *Int. J. Mass Spec.* **2006**, *254*, 1–19.
(28) Polfer, N. C.; Oomens, J.; Suhai, S.; Paizs, B. *J. Am. Chem. Soc.* **2007**, *129*, 5887–5897.
(29) Correia, C. F.; Balaj, P. O.; Scuderi, D.; Maitre, P.; Ohanessian, G. *J. Am. Chem. Soc.* **2008**, *130*, 3359–3370.
(30) Simon, A.; MacAleese, L.; Maitre, P.; Lemaire, J.; McMahon, T. B. *J. Am. Chem. Soc.* **2007**, *129*, 2829–2840.
(31) Wu, R.; McMahon, T. B. *J. Am. Chem. Soc.* **2007**, *129*, 11312–11313.
(32) Oomens, J.; Tielens, A.; G, G. M.; Sartakov, B. G.; Von Helden, G.; Meijer, G. *Astrophys. J.* **2003**, *591*, 968–985.
(33) Chellgren, B. W.; Creamer, T. P. *Proteins* **2006**, *62*, 411–420.

by cluster analysis and DFT calculations, are used to predict energetically favored structures. These predictions are initially interpreted in terms of the C_n notation of Mons and coworkers,[16] where n is the number of atoms involved in an intramolecular hydrogen bond, as this interpretation has allowed the clearest connection between IR spectroscopic signatures and traditional peptide structural motifs. However, due to the complexity of the present system, the hydrogen-bonding configurations are not always simple, and precise C_n spectroscopic assignments are not always possible. Nevertheless, some amount of conformational information can often be obtained. In the present work, the neutral peptide, studied under cold molecular beam conditions with IR/UV double-resonance spectroscopy, exhibits two half-β-strands with a C_{10} β-turn in the middle of the peptide. The influence of ionic forces via protonation at the lysine is demonstrated in the protonated peptide, Ac-VQIVYK(H^+)-NHMe, through analysis of the amide I/II bands obtained with IRMPD spectroscopy using the FTICR mass spectrometer apparatus[28,34] at the FELIX IR source in The Netherlands. In the protonated tau-peptide fragment, the lysine NH_3^+ binds to the peptide backbone and completely alters the neutral β-strand/β-turn conformation into a random-coil-like structure.

Experimental Details

Characterization of Neutral Peptide. The capped peptide Ac-VQIVYK-NHMe was chosen to model the ^{306}VQIVYK^{311} sequence because it should have minimal interaction between the C-terminal cap (NHMe) and the rest of the peptide. Ac-VQIVYK-NHMe was obtained from Celtek Peptides. The neutral Ac-VQIVYK-NHMe peptide was characterized in the gas phase using IR/UV double-resonance spectroscopy.[19] Our instrumental setup has been described previously,[35] and only a summary is given here. The solid sample was mixed with graphite powder in a ratio of ~80% sample to 20% graphite (by volume) and coated onto a rotating graphite rod situated near the conical nozzle of a pulsed valve (General Valve). The sample was vaporized by laser desorption of the graphite rod, using the 1064 nm output of a Continuum Minilite Nd:YAG laser (0.5 mJ/pulse). The peptide molecules were then cooled in a pulsed argon molecular beam and passed through a skimmer (Beam Dynamics, 3 mm) into a linear time-of-flight (TOF) mass spectrometer (Jordan). Previous rotational band contour analyses have suggested a rotational temperature of ~5−10 K in our instrument,[36,37] although due to the laser desorption this value may be slightly higher in the present work. Meijer et al. have reported a vibrational temperature of 15 K for diphenylamine in a molecular beam after laser desorption,[38] but the Ac-VQIVYK-NHMe vibrational temperature may be significantly higher for this relatively large molecule due to less efficient vibrational cooling. We cannot quantify the exact temperatures due to the lack of UV spectral resolution (vide infra). The cold peptides were ionized via the tyrosine chromophore by resonant two-photon ionization (R2PI), using the frequency-doubled output of a Lambda Physik FL2002 dye laser, pumped with the 355 nm output of a Surelite III Nd:YAG laser. For the IR spectroscopy, the idler output of a Laservision KTP/KTA OPO/OPA system (bandwidth ~2−3 cm^{-1}), pumped by a Surelite II Nd:YAG laser, was used as a hole-burning laser, irradiating the molecules 100 ns before the R2PI laser. The IR/UV double-resonance technique has been discussed in detail elsewhere.[39] The IR spectrum was recorded by monitoring the depletion of the peptide ion signal in the mass spectrometer as a function of IR frequency between 2800 and 3700 cm^{-1} (corresponding to the OH, NH, and CH stretch regions). Active baseline correction was employed to accommodate signal fluctuations: the experiment operated at 10 Hz while the IR laser operated at 5 Hz.

Characterization of Protonated Peptide. Experiments on the protonated peptide were conducted at the FELIX free electron laser (FEL) facility of the FOM Institute for Plasma Physics in Nieuwegein, NL. The capped protonated ^{306}VQIVYK^{311} sequence, Ac-VQIVYK(H^+)-NHMe, was analyzed in an ESI-FTICR mass spectrometer, for which details have been published elsewhere.[28,34] The spray was operated using a 1.6 mM solution of the peptide in 50:50 H_2O:MeOH (by volume). The protonated ion was accumulated in a hexapole RF trap and was then pulse-injected into the FTICR mass spectrometer via a quadrupole deflector and an octopole ion guide. The parent ion (m/z = 804) was isolated in the FTICR using SWIFT excitation and subsequently irradiated by the mid-IR output of the FEL (described in detail elsewhere[40]) for 2 s. When the FEL was on-resonance with a peptide vibrational transition (for example, the amide I band, vide infra), the ion dissociated (via IRMPD[27]) into ions of m/z 482 and 142 with a branching ratio of roughly 4:1; the peptide fragmentation is not discussed further in this work. The IRMPD spectrum was recorded by monitoring the percent fragmentation of the peptide as a function of FEL frequency from 800 to 1800 cm^{-1} (corresponding to the amide I/II band region as well as the fingerprint region).

Computational Details. Initial conformations for both the neutral and protonated peptides were generated by a molecular-mechanics-based Monte-Carlo multiple minimization (MCMM) using the MacroModel program[41] as implemented in Maestro.[42] The AMBER* force field, developed for peptide backbone conformations,[43] was used for all conformational searches and minimizations. Conformers were generated within a 50 kJ/mol window using a maximum of 5000 iterations, each with a maximum of 10 000 MCMM steps. To eliminate any duplicate structures, a multiple minimization step was carried out on the structures produced in the conformational search, with a maximum of 5000 iterations and a cutoff energy of 50 kJ/mol. This two-step process was repeated iteratively until no new low-energy conformers were found.

The structures generated from the above procedure were analyzed with cluster analysis (with the XCluster software,[44] also included in Maestro) in order to ensure only unique low-energy conformations were submitted for DFT calculations. The conformational searches generated hundreds of low-energy conformers, but most of these fall into one of a few discrete structural families. Within these families the backbone conformations are the same and side-chain conformational differences are either negligible (e.g., slight differences in the Gln position) or not important (e.g., differences in Val CH_3 group rotations). The XCluster analysis provides a statistical procedure to sort these families, and both the neutral and protonated peptides produced only a handful of discrete structures, which were then subjected to optimization and harmonic frequency calculation at the B3LYP/6-31G(d) level. While more accurate structure/frequency calculations for this large molecule (122 atoms) would be prohibitively expensive, single-point energy calculations

(34) Valle, J. J.; Eyler, J. R.; Oomens, J.; Moore, D. T.; van der Meer, A. F. G.; Von Helden, G.; Meijer, G.; Hendrickson, C. L.; Marshall, A. G.; Blakney, G. T. *Rev. Sci. Instrum.* **2005**, *76*, 023103.
(35) Carcabal, P.; Hunig, I.; Gamblin, D. P.; Liu, B.; Jockusch, R. A.; Kroemer, R. T.; Snoek, L. C.; Fairbanks, A. J.; Davis, B. G.; Simons, J. P. *J. Am. Chem. Soc.* **2006**, *128*, 1976–1981.
(36) Lee, Y.; Jung, J.; Kim, B.; Butz, P.; Snoek, L. C.; Kroemer, R. T.; Simons, J. P. *J. Phys. Chem. A* **2004**, *108*, 69–73.
(37) Snoek, L. C.; van Mourik, T.; Simons, J. P. *Mol. Phys.* **2003**, *101*, 1239–1248.
(38) Meijer, G.; de Vries, M. S.; Hunziker, H. E.; Wendt, H. R. *Appl. Phys. B: Laser Opt.* **1990**, *51*, 395–403.
(39) Zwier, T. S. *J. Phys. Chem. A* **2001**, *105*, 8827–8839.
(40) Oepts, D.; Van der Meer, A. F. G.; Van Amersfoort, P. W. *Infrared Phys. Technol.* **1995**, *36*, 297–308.
(41) Mohamadi, F.; Richards, N. G. J.; Guida, W. C.; Liskamp, R.; Lipton, M.; Caufield, C.; Chang, G.; Hendrickson, T.; Still, W. C. *J. Comput. Chem.* **1990**, *11*, 440–467.
(42) Maestro, 1.2.014 ed.; Schrodinger, L.L.C., 1999.
(43) McDonald, D. Q.; Still, W. C. *Tetrahedron Lett.* **1992**, *33*, 7743–7746.
(44) Shenkin, P. S.; McDonald, D. Q. *J. Comput. Chem.* **1994**, *8*, 899–916.

were computed for the B3LYP/6-31G(d) structures at the B3LYP/6-311++G(d,p) level in order to estimate better the relative energies. An important note here is that the neglect of dispersion energy by the B3LYP functional may cause errors in predicting the Tyr side chain conformation. Therefore, we also computed single-point energies for the B3LYP/6-31G(d) structures using the M05-2X functional (with the 6-311++G(d,p) basis set), which should at least treat the dispersion interaction more accurately.[45] All energies were corrected for ZPE using the unscaled harmonic B3LYP/6-31G(d) frequencies. While the neutral peptide was characterized under cold conditions, the protonated peptide ion was characterized at 298 K. Therefore, for the Ac-VQIVYK(H^+)-NHMe, free energies were computed using the unscaled B3LYP/6-31G(d) frequencies for enthalpic and entropic contributions. All DFT calculations were performed with Gaussian 03 software.[46]

Results and Discussion

Neutral Ac-VQIVYK-NHMe. Computational Results. We begin with a discussion of the predicted favorable conformations based on the computational procedure outlined above. For the neutral Ac-VQIVYK-NHMe, only four unique conformations (within the lowest 100 conformers found from the conformational search) were generated from the cluster analysis outlined above. The DFT-optimized structures for these four conformations (**N1**−**N4**) are shown in Figure 2, and the relative energies are summarized in Table 1. While the energetic ordering does not change from the B3LYP/6-31G(d) to B3LYP/6-311++G(d,p) level, it does change with the M05-2X/6-311++G(d,p) calculations: conformer **N3** changes from being unfavorable by 21.2 kJ/mol to being the most favorable by 7.5 kJ/mol. The most favorable neutral structure from the B3LYP calculations, conformer **N1**, presents a C_7 hydrogen bond (that is, a γ-turn) around the Ile-Val-Tyr sequence, while the other two halves of the peptide backbone are relatively straight, with an NH→O═C hydrogen bond between the Ile and the Lys backbones. Also evident are interactions between the side chains (shown only as thin wires in Figure 2A) and the backbone: the Tyr OH binds to the Val C═O while the Gln NH binds to the Ile C═O. These different hydrogen-bonding interactions are shown schematically for all four conformers in Figure 2B. An important note here is that the neglect of dispersion energy by the B3LYP functional may cause errors in predicting the Tyr side chain conformation, although the predictions for the backbone and remaining residues are likely of reasonable qualitative accuracy.

Conformer **N2** presents a C_7 interaction (Gln-Ile-Val) but also clearly has a C_{10} interaction surrounding the Ile and Val. While the NH→O═C C_{10} interaction appears bent or skewed, the backbone conformation clearly represents a β-turn *motif* and the two peptide halves form quite straight chains. Notably, while the Gln and Lys appear to interact in some way with the backbone, the Tyr OH is free. With both the B3LYP and M05-2X calculations, this β-hairpin-like conformer is only slightly less favorable (less than 4 kJ/mol) than **N1** (Table 1). The remaining two neutral conformers, **N3** and **N4**, are similar to **N1** and **N2**, respectively. **N3** is similar to **N1**, with a C_7 γ-turn, but involving Gln-Ile-Val instead of Ile-Val-Tyr. **N3** also exhibits a backbone NH→O═C interaction between the acetyl cap and the Lys NH, as well as a Tyr OH hydrogen bonded to a backbone carbonyl. **N4** is similar to **N2**, with a C_{10} β-turn, two β-strand-like halves, and a free Tyr OH. However, the two β-strand chains are not in a perfect hairpin, as with **N2**, but rather bend away from each other. While **N3** is predicted to be quite favorable with the M05-2X/6-311++G(d,p) calculations, **N4** is predicted to be unfavorable by over 20 kJ/mol at all levels of theory considered.

The computational results for the neutral peptide thus predict four rather similar conformations. All four (**N1**−**N4**) are essentially extended peptides bent into two halves by either a γ-turn (**N1**, **N3**) or a β-turn (**N2**, **N4**). The two halves are somewhat twisted in **N1** and **N3**, possibly due to the Tyr OH interaction, while in **N2** they are straighter, as the β-turn (and perhaps the lack of Tyr OH hydrogen bonding) allows them to interact better with one another. The β-strands in **N4** appear to be straight, but are bent away from each other. In any case, from the energies in Table 1, it is clear that despite the overall similarity of the predicted conformers, the more subtle differences, both in the peptide backbone conformations and in the side chain−backbone interactions, result in fairly large energy differences, although the differences involving **N3** change depending on the DFT functional used. Thus, the actual preferred neutral peptide conformation is likely the result of a complex and subtle interplay between many different types of intramolecular interactions.

Experimental Results. The neutral Ac-VQIVYK-NHMe R2PI spectrum was scanned in the UV absorption region of tyrosine[47] and other tyrosine-containing peptides,[48] that is, 280−283 nm. While the detection of parent peptide ions from the R2PI laser clearly indicates UV absorption in this region, we were unable to resolve any features in the UV band (which is very broad; not shown). This is likely due to a combination of several factors, including large shot-to-shot fluctuations in ion signal, warm vibrational temperatures, and possibly UV band saturation (among other factors), although spectral features remained unresolved at lower R2PI laser fluence. Excited state dynamics do not likely contribute to UV broadening, as tyrosine is known to have relatively long excited-state lifetimes.[49] In any case, lack of UV spectral resolution prevented the use of UV/UV double-resonance techniques to identify unambiguously different conformers. Therefore, we recorded the IR spectrum at three different probe wavelengths (281.6, 282.1, 282.6 nm). No significant differences were observed between these three spectra, implying either that there is only a single conformer or a combination of conformations present at all UV probe wavelengths. Only the best spectrum, recorded with the UV at 282.1 nm, is analyzed here; this spectrum is shown at the top of Figure 3.

The IR spectrum displays hydride stretching bands in three clearly distinct spectral regions. The band at 3655 cm^{-1} most likely corresponds to the free tyrosine OH stretch, as it is very near the free OH stretch of both phenol[50] and tyrosine.[49] This immediately indicates that the Tyr OH in the Ac-VQIVYK-NHMe peptide is not involved in hydrogen bonding. The bands between 3500 and 3300 cm^{-1} most likely correspond to NH stretches (both free and hydrogen-bonded) based on comparison to published spectra.[17,19,20,23,48] They could contain hydrogen-bonded OH band(s), but the observation of a free OH band

(45) Zhao, Y.; Schultz, N. E.; Truhlar, D. G. *J. Chem. Theory Comput.* **2006**, *2*, 364–382.
(46) Frisch, M. J.; et al. Gaussian, Inc: Pittsburgh, PA, 2003.
(47) Martinez, S. J., III.; Alfano, J. C.; Levy, D. H. *J. Mol. Spectrosc.* **1992**, *156*, 421–430.
(48) Fricke, H.; Gerlach, A.; Unterberg, C.; Rzepecki, R.; Schrader, T.; Gerhards, M. *Phys. Chem. Chem. Phys.* **2004**, *6*, 4636–4641.
(49) Inokuchi, Y.; Kobayashi, Y.; Ito, T.; Ebata, T. *J. Phys. Chem. A* **2007**, 111.
(50) Ebata, T.; Fujii, A.; Mikami, N. *Int. J. Mass Spec. Ion Proc.* **1996**, *159*, 111–124.

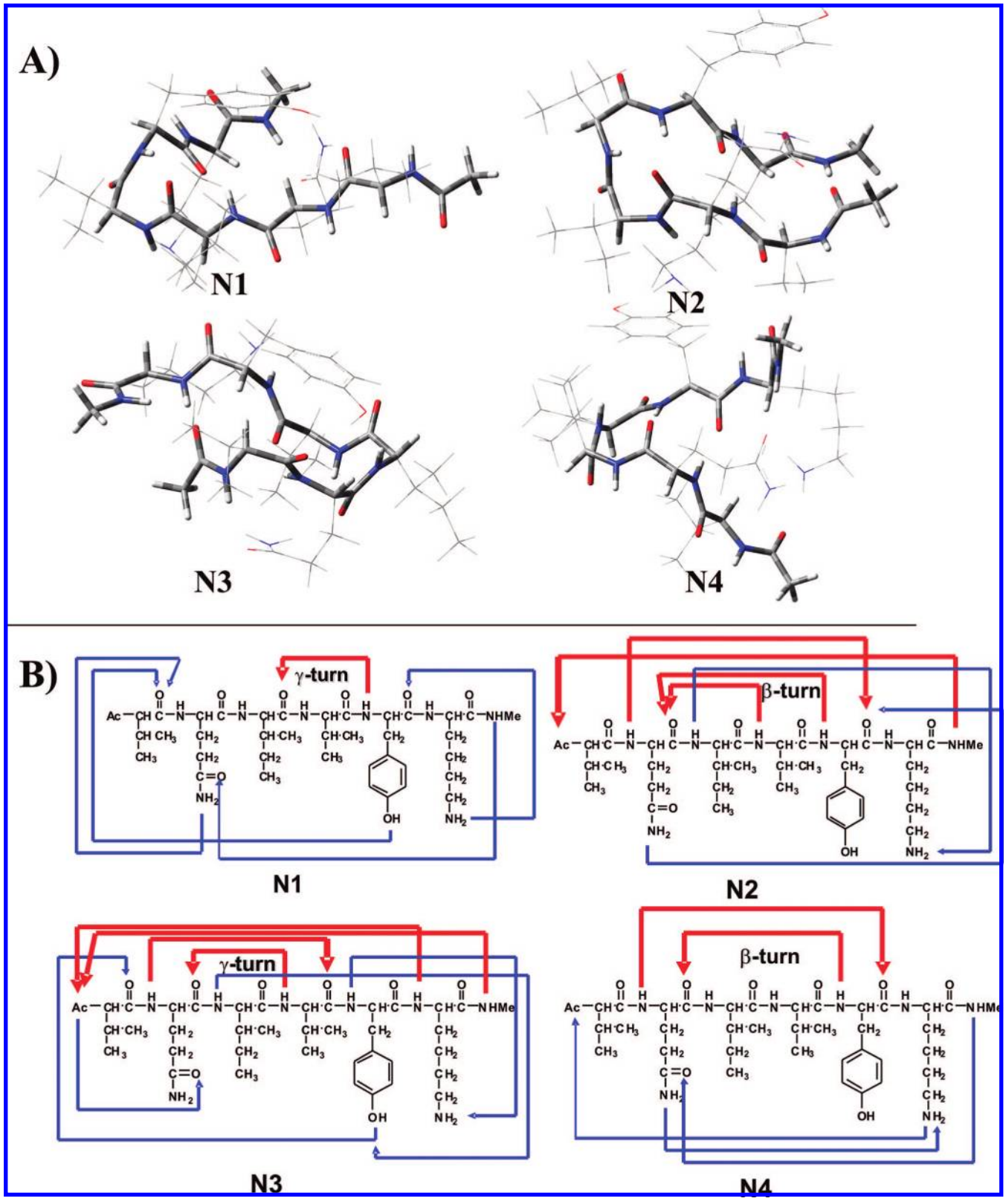

Figure 2. Structures of the four low-energy conformers for neutral Ac-VQIVYK-NHMe predicted by the theoretical investigation. See the text for detailed descriptions of the structures in terms of the backbone conformations. (A) Molecular representations of the peptide structures, with the amino acid side chains displayed as thin wires to emphasize the predicted backbone conformations. (B) Schematic representations of the structures in terms of the intramolecular hydrogen bonds predicted. Intramolecular hydrogen bonds are shown as arrows from H-bond donor to acceptor. The H-bond donor on the acetyl cap is the NH, while the acceptor is the C=O (not shown). Interactions involving only the backbone are shown as thick red lines, while interactions between side chain and backbone, or between side chains, are shown as thin blue lines.

makes this unlikely (though the spectrum is not truly conformer-specific). The intense bands below 3000 cm^{-1} could correspond either to strongly hydrogen-bonded (OH or NH) modes or CH stretch modes. While CH stretch modes are typically quite weak,

Table 1. Relative Energies (ΔE in kJ/mol) for the Four Conformations of the Neutral Ac-VQIVYK-NHMe Predicted by the Theoretical Investigation

	ΔE		
conformer	B3LYP/6-31G(d)[a]	B3LYP/6-311++G(d,p)//B3LYP/6-31G(d)[b]	M05-2X/6-311++G(d,p)//B3LYP/6-31G(d)[c]
N1	0.0	0.0	7.5
N2	11.9	3.3	10.9
N3	12.2	21.2	0.0
N4	25.3	23.0	26.5

[a] Computed with B3LYP/6-31G(d) energies, using unscaled B3LYP/6-31G(d) frequencies for ZPE corrections. [b] Computed with B3LYP/6-311++G(d,p)//B3LYP/6-31G(d) single-point energies, using unscaled B3LYP/6-31G(d) frequencies for ZPE corrections. [c] Computed with M05-2X/6-311++G(d,p)//B3LYP/6-31G(d) single-point energies, using unscaled B3LYP/6-31G(d) frequencies for ZPE corrections.

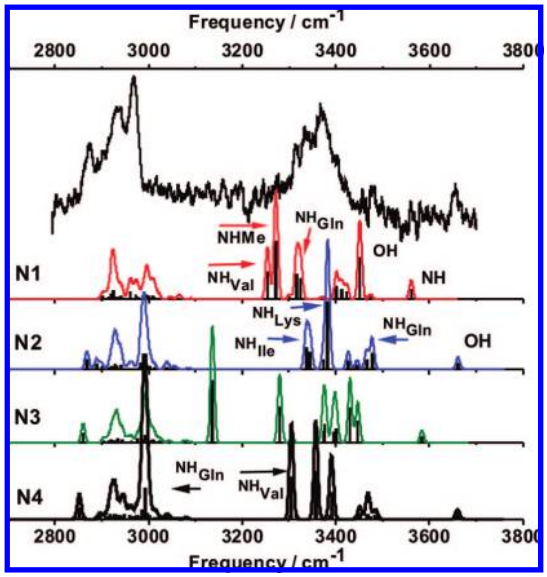

Figure 3. Experimental IR spectrum of the neutral capped VQIVYK (top), recorded using IR/UV hole-burning spectroscopy with an R2PI probe wavelength of 282.1 nm. IR spectra recorded at different R2PI wavelengths are identical. The weak spectral feature at 3477 cm^{-1} is reproducible, while the features around 3200 cm^{-1} are not. Included for comparison to theory are the theoretical IR spectra for each of the conformers in Figure 2. The harmonic DFT frequencies are scaled by 0.976 and 0.96 for the OH and NH/CH stretch modes, respectively (see the text). The computed spectra are shown both as stick spectra and convolved with a Gaussian line shape (10 cm^{-1} fwhm). Vibrational mode assignments are noted for some of the more intense bands in **N1**, **N2**, and **N4**.

the Ac-VQIVYK-NHMe peptide has 53 CH groups, and therefore, it is likely that the bands below 3000 cm^{-1} arise (at least in part) from CH modes. As an important note, the overall structure of the isolated, gas-phase Ac-VQIVYK-NHMe IR spectrum is very similar to that reported for gas-phase gramicidin S,[18] a cyclic decapeptide that forms an intramolecular β-sheet.[51]

For comparison between the experimental and theoretical results, the computed IR spectra (frequencies and relative IR intensities, convolved with a 10 cm^{-1} fwhm Gaussian profile to match experimental line shapes, based on the free Tyr OH band) for each of the four predicted conformers are shown below the experimental IR spectrum in Figure 3. The harmonic B3LYP/6-31G(d) frequencies are scaled by 0.976 for the OH stretch mode (ratio of experimental[50] to computed OH stretch for phenol) and 0.96 for the NH (and CH) modes (as recommended by Merrick et al.[52]). All frequencies below are reported after scaling. In the computed **N1** spectrum there is a free NH band, corresponding to the acetyl cap NH, at 3560 cm^{-1}, and the hydrogen-bonded OH band at 3449 cm^{-1}. Free and weakly hydrogen-bonded NH modes are predicted around 3400 cm^{-1}, and hydrogen-bonded NH modes from the Gln NH as well as backbone NH groups (from the NHMe cap and the Val NH) are predicted below 3350 cm^{-1}. All predicted bands below 3000 cm^{-1} correspond to CH stretch modes.

It is immediately clear that the computed **N1** spectrum does not agree particularly well with the experiment, especially regarding the lack of a predicted free OH stretch. Also there are clearly no intense bands between 3200 and 3300 cm^{-1} in the experiment, although predicted by the calculation. While we cannot discount the possibility of a minor contribution from **N1**, this is not likely the dominant conformer. The computed **N2** spectrum predicts a free OH at 3659 cm^{-1}, a free Gln NH at 3477 cm^{-1}, and many free and weakly hydrogen-bonded NH modes between 3400 and 3500 cm^{-1}. Included in this region is the C_{10} (β-turn) hydrogen-bonded NH stretch, which is not strongly shifted to lower frequency because the H-bond distance is not short enough (slightly over 4 Å; see Figure 2). The intense hydrogen-bonded NH stretching bands at 3337 and 3382 cm^{-1} correspond to the Ile NH (interacting with the Lys NH_2) and the Lys NH_2 asymmetric stretch, respectively. Thus, based on the relationship between hydrogen-bond strength and vibrational frequency (and IR intensity), the NH→O=C interactions are not predicted to be particularly strong. In any case, the computed **N2** spectrum appears to agree much better with the experiment than **N1**. Notably, the free OH band is predicted almost exactly, and the predicted CH bands (after convolution) fit the experimental bands below 3000 cm^{-1} nearly perfectly, at least with respect to the observed band shapes. Note that the absolute frequencies of these CH bands are probably not predicted exactly because of slight inadequacies in the scaling factor. Also, the weak spectral feature observed (experimentally) at 3477 cm^{-1}, which appears to agree with the predicted Gln NH from **N2**, is reproducible (note that the experimental features of similar intensity below 3200 cm^{-1} are not reproducible).

While the **N3** predicted spectrum does not agree with the experiment at all, despite its low M05-2X/6-311++G(d,p) energy, the computed **N4** spectrum appears to agree almost as well as that of **N2**. In the **N4** spectrum, there is an intense hydrogen-bonded NH at 2989 cm^{-1} (from the Gln as noted in Figure 3) that could contribute to the experimental band at 2967 cm^{-1}, although this feature can in principle be completely explained on the basis of the **N2** spectrum. Also noted in the predicted **N4** spectrum is a hydrogen-bonded backbone NH at 3302 cm^{-1} (NH_{Val}) that could contribute to the experimental band between 3300 and 3400 cm^{-1}. The similarity between the computed **N2** and **N4** is not surprising as the structures are very similar; see Figure 2. However, the energy of **N4** (Table 1) is more than 20 kJ/mol higher than the global minimum (**N1** or **N3** depending on the DFT functional), while **N2** is only slightly higher. It is therefore clear from the analysis that the peptide adopts the β-turn conformation (either **N2** or **N4**), and we conclude on the basis of both the agreement between theoretical and experimental spectra and computed energies that **N2** represents the dominant conformation of the neutral Ac-VQIVYK-NHMe.

(51) Krauss, E. M.; Chan, S. I. *J. Am. Chem. Soc.* **1982**, *104*, 6953–6961.

(52) Merrick, J. P.; Moran, D.; Radom, L. *J. Phys. Chem. A* **2007**, *111*, 11683–11700.

Effect of Lysine Protonation: Ac-VQIVYK(H^+)-NHMe. Computational Results. Under physiological conditions, the lysine side chain of Ac-VQIVYK-NHMe will most likely be protonated, and it is therefore important to understand the effect of the strong cationic forces from the Lys NH_3^+ on the inherent peptide conformation. We therefore proceed to discuss the conformational landscape of the Ac-VQIVYK(H^+)-NHMe cation. Protonation will occur at the Lys side chain, as the pK_b of the side chain NH_2 ($\sim$3.5)[53] is much lower than that of the amide NH groups ($\geq$14);[54] we did not consider different protonation sites in our theoretical investigation. We identified eight unique conformations of Ac-VQIVYK(H^+)-NHMe from the lowest 50 AMBER* conformers, but here we only discuss the four lowest-energy conformers, which fall in a 25 kJ/mol window at the DFT level. This is justifiable, because the fifth-lowest-energy conformer is more than 35 kJ/mol higher than the global minimum. The four conformers are shown in Figure 4 in both their molecular representations (Figure 4A) and hydrogen-bonding schematic representations (Figure 4B). All eight conformers are included in Figure S1 of the Supporting Information.

As discussed above, the protonated peptide was characterized at 298 K, and therefore both the relative energies (ΔE) and free energies (ΔG_{298}) are summarized for the four lowest-energy conformations, **P1**−**P4**, in Table 2. While the entropies computed using the unscaled DFT frequencies are probably quantitatively inaccurate due to the highly anharmonic nature of the low-frequency vibrations (which contribute most to the entropy), the entropic differences between the conformers are likely qualitatively accurate and, as a result of the conformational similarities evident in Figure 4, small. With the B3LYP calculations, the energetic ordering of the four conformations does not change from 0 to 298 K because the entropic content of all conformers is similar and the relative (0 K) energy differences are quite large. As with the neutral Ac-VQIVYK-NHMe, the ordering changes somewhat with the M05-2X functional in that **P4** becomes more favorable by $\sim$20 kJ/mol. Notably, with the M05-2X functional, **P4** is the lowest-energy conformer (at 0 K), but at 298 K it is slightly unfavorable (by 0.7 kJ/mol). In conformer **P1**, the Lys side chain is folded back, and all three protons of the NH_3^+ group bind to backbone C═O groups. The peptide backbone itself appears helical, with a C_{15} NH→O═C interaction and a (bent) C_{13} (α-helical) interaction. This structure is dramatically different from the observed neutral Ac-VQIVYK-NHMe conformer, **N2**. In **P1**, protonation at the Lys side chain induces a transition from a β-hairpin-like structure to a helical structure as a result of the NH_3^+−backbone interactions.

Conformer **P2** appears similar to **P1**: The Lys NH_3^+ group interacts with three peptide C═O groups to distort the backbone conformation. However, the remaining backbone does not adopt a helical configuration, because the Gln interacts with the peptide backbone in both H-bond donor (NH_2) and acceptor (C═O) modes. From Table 2, this conformation is less favorable than that of **P1** with both the B3LYP and M05-2X functionals. In **P3**, which is clearly different from **P1** and **P2**, the Lys NH_3^+ interacts with only two peptide C═O groups, while the Gln NH_2 acts as a double H-bond donor to both the acetyl and NHMe caps. **P4** appears very similar to **P1**, where the Lys NH_3^+ is involved in hydrogen bonds with three C═O groups and the rest of the peptide backbone appears relatively free and unfolded. Thus, it is not too surprising that, with the M05-2X energies in Table 2, this conformer is energetically close to **P1**. Note that while **P4** does present a C_{13} interaction (Figure 4B), the peptide conformation can hardly be described as helical.

The computational results for the protonated peptide predict a preferred conformational family where the Lys NH_3^+ binds to the backbone carbonyl groups and the backbone itself adopts a random coil conformation. While the energy ordering between the first four conformers is debatable, because of the changes between the B3LYP and M05-2X calculations, it is clear that conformers in which the NH_3^+ interacts with three backbone carbonyls (**P1**, **P2**, and, with the M05-2X calculations, **P4**) are more favorable than **P3**, in which only two carbonyls are bound.

Experimental Results. The IRMPD spectrum of the Ac-VQIVYK(H^+)-NHMe peptide ion is shown at the top of Figure 5. The entire spectrum is shown in Figure 5A, while the amide I band only is shown in Figure 5B. The most intense features are the amide I band at $\sim$1670 cm^{-1}, corresponding to modes of mostly C═O stretch character, and the amide II band at $\sim$1520 cm^{-1}, corresponding to modes of mostly NH bending character. The weak band at 1595 cm^{-1} could arise from either a strongly red-shifted C═O mode, an unusually high-frequency NH bending mode, or a mode related to the NH_3^+ group. The broad nature of the IRMPD bands, reflecting in part the large number of vibrational modes present, makes it difficult to speculate about conformational assignments based solely on the experiment. It is worth noting, however, that the amide I value (1670 cm^{-1}) suggests a randomly coiled, relatively unfolded peptide based on FTIR investigations of solution-phase sequences.[11]

Nevertheless, the IRMPD spectrum cannot be interpreted in detail without the help of theory. The computed spectra for the four conformers from Figure 4 are shown below the experiment in Figure 5A. The predicted spectra are taken from the computed frequencies and relative IR intensities, convolved with Gaussian profiles with a fwhm width equal to 0.5% of $1/\lambda$ (as the FEL bandwidth is inversely proportional to wavelength, λ). All eight conformers are included in Figure S2 of the Supporting Information. The harmonic DFT frequencies are scaled by 0.965, which has been used previously for B3LYP/6-31G(d) frequencies in this spectral region.[28] Note that this scaling factor also corrects for the slight shifts between single-photon and multiple-photon IR band positions. For **P1**, a group of C═O modes is predicted around 1660 cm^{-1}, with a single intense C═O stretch (corresponding to the Gln C═O interacting with the acetyl cap) at 1700 cm^{-1}. The predicted band at 1570 cm^{-1} corresponds to the NH_3^+ umbrella mode, and not surprisingly, the NH bending modes are predicted around $\sim$1518 cm^{-1}. The computed spectra for **P2**−**P4** have similar mode assignments, although there are notable (albeit subtle) differences between the four computed spectra. These differences are mostly clearly highlighted in the convolved theoretical spectra.

Upon close comparison between the different (convolved) computed spectra, it appears that the **P1** spectrum most closely agrees with the experiment. First, only **P1** predicts an amide II band at 1518 cm^{-1} (experiment is 1520 cm^{-1}); the other three predict the amide II band at $\sim$1510 cm^{-1}. Also, the fingerprint IR bands below 1400 cm^{-1} are best predicted by **P1**. The experimental band at 1595 cm^{-1} is not quantitatively reproduced by the predicted **P1** spectrum, but based on the shape and relative intensity, the predicted band at 1573 cm^{-1} could be assigned to this feature, given the assumption that this vibration

(53) Ellenbogen, E. *J. Am. Chem. Soc.* **1952**, *74*, 5198.
(54) *Handbook of Chemistry and Physics*; Hodgman, C. D., Ed.; Chemical Rubber Co.: Cleveland, OH, 1951.

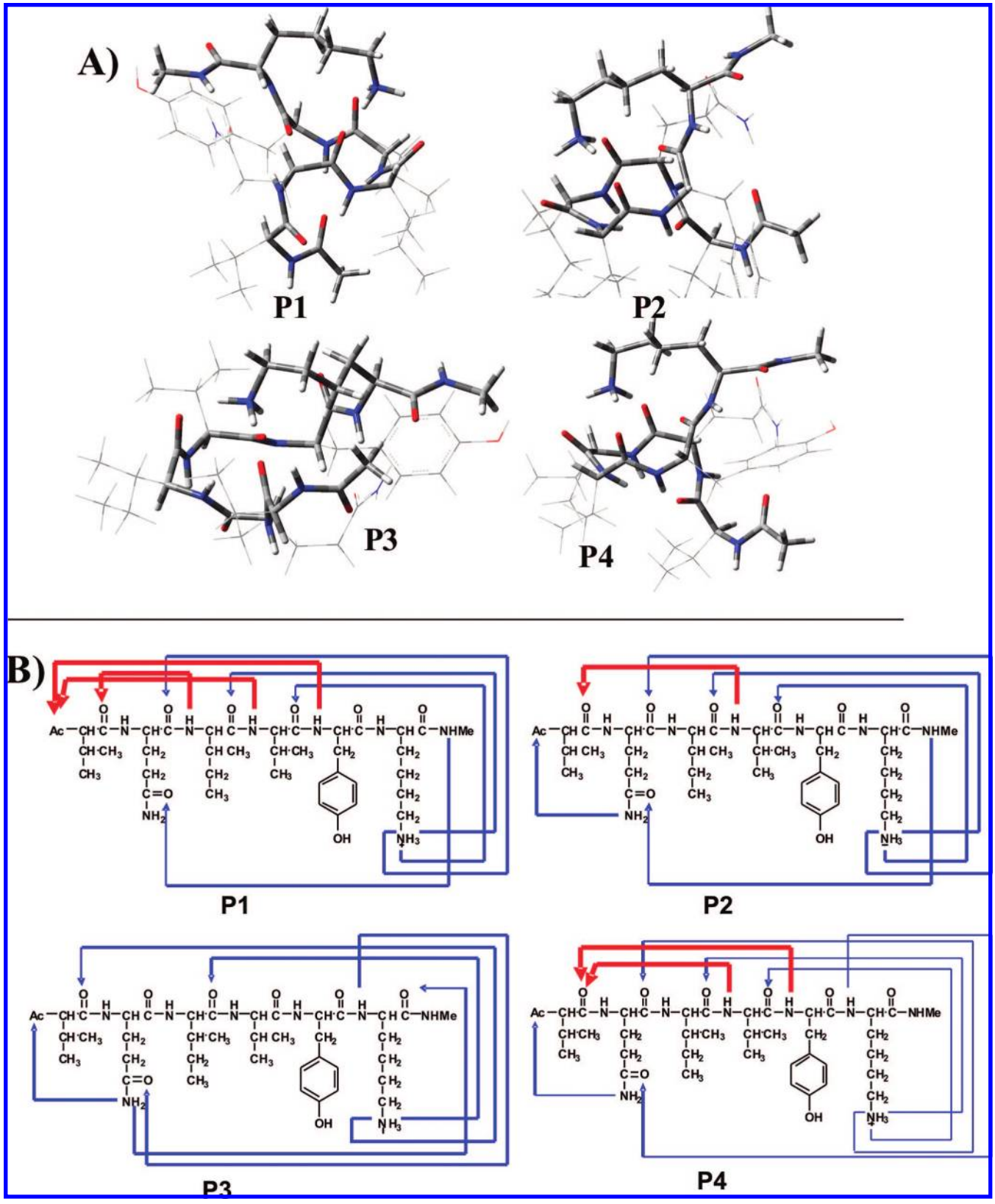

Figure 4. Structures of the four low-energy conformers for the protonated peptide Ac-VQIVYK(H^+)-NHMe predicted by the theoretical investigation. See the text for detailed descriptions of the structures in terms of the backbone conformations. (A) Molecular representations of the peptide structures, with the amino acid side chains displayed as very thin wires to emphasize the predicted backbone conformations. (B) Schematic representations of the structures in terms of the intramolecular hydrogen bonds predicted. Intramolecular hydrogen bonds are shown as arrows from H-bond donor to acceptor. The H-bond donor on the acetyl cap is the NH, while the acceptor is the C═O (not shown). Interactions involving only the backbone are shown as thick red lines, while interactions between side chain and backbone, or between side chains, are shown as thin blue lines.

Table 2. Relative Energies and 298 K Free Energies (ΔE and ΔG_{298}, respectively, in kJ/mol) for the Four Conformations of the Protonated Ac-VQIVYK(H^+)-NHMe Predicted by the Theoretical Investigation

	B3LYP/6-31G(d)[a]		B3LYP/6-311++G(d,p)//B3LYP/6-31G(d)[b]		M05-2X/6-311++G(d,p)//B3LYP/6-31G(d)[c]	
conformer	ΔE	ΔG_{298}	ΔE	ΔG_{298}	ΔE	ΔG_{298}
P1	0.0	0.0	0.0	0.0	4.0	0.0
P2	6.8	5.5	10.8	9.5	7.8	2.5
P3	11.2	15.0	15.6	19.4	21.8	21.8
P4	22.5	13.5	16.7	21.5	0.0	0.7

[a] Computed with B3LYP/6-31G(d) energies, using unscaled B3LYP/6-31G(d) frequencies for ZPE and free-energy corrections. [b] Computed with B3LYP/6-311++G(d,p)//B3LYP/6-31G(d) single-point energies, using unscaled B3LYP/6-31G(d) frequencies for ZPE and free-energy corrections. [c] Computed with M05-2X/6-311++G(d,p)//B3LYP/6-31G(d) single-point energies, using unscaled B3LYP/6-31G(d) frequencies for ZPE and free-energy corrections.

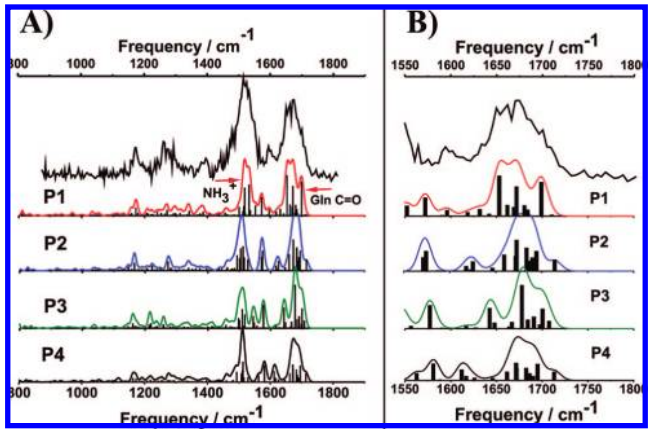

Figure 5. (A) Experimental IRMPD spectrum of protonated Ac-VQIVYK(H^+)-NHMe (top) recorded in the ESI-FTICR mass spectrometer using an IR FEL. The intense features at 1670 and 1520 cm^{-1} correspond to the amide I and II bands, repectively. Included for comparison to theory are the theoretical IR spectra for each of the conformers in Figure 4. The harmonic DFT frequencies are scaled by 0.965. The computed spectra are shown both as stick spectra and convolved with a Gaussian line shape to match the FEL line shape (1% of FEL wavelength fwhm). Vibrational mode assignments are noted for a few of the bands in **P1**. (B) Expanded view of the amide I region of the Ac-VQIVYK(H^+)-NHMe IRMPD spectrum (top). Shown below the experiment are the predicted amide I bands for the four conformers **P1**−**P4**.

is not as well-treated by the current theory. Notably, this 1595 cm^{-1} IRMPD band is not reproduced by any conformer in Figure 5 or Figure S2 of the Supporting Information. To highlight the agreement between the predicted **P1** spectrum and the experiment, an expanded view of the amide I region is shown in Figure 5B. While differences between the four computed amide I bands are subtle, it is clear that the **P1** prediction matches best.

While the computed B3LYP ΔE and ΔG_{298} values in Table 2 suggest that **P1** is the only favorable conformation, the M05-2X values suggest that **P2** and **P4** are also favorable. The predicted spectra for these two conformers also seem to agree somewhat with the IRMPD spectrum. This is not too surprising, given the similarity between these three conformers (see Figure 4). As discussed in the Introduction, the idea of peptide conformations in this 298 K experiment is different from that of the cold neutral peptides. Given the quality of fit between the predicted and experimental spectrum, it is likely that **P1** is representative of the average Ac-VQIVYK(H^+)-NHMe peptide conformation, while dynamic interconversion between **P2** and **P4** (and possibly even **P3**) occurs on the experiment time scale. Indeed, this would be consistent with the moderate and large-amplitude motions of the side chains investigated by Chellgren and Creamer[33] as well as Gregoire et al.,[55] as the main differences between **P2** and **P4** involve changes in the side-chain conformations.

Given the available experimental data, that is, the IRMPD spectrum in the amide I/II band region, there is clearly some ambiguity remaining in the spectral interpretation of Figure 5. In this context, it would be highly informative to record the IRMPD spectrum in the OH/NH/CH stretch region and compare the hydrogen-bonded NH stretch modes of the Lys NH_3^+ as well as the backbone amide groups. Furthermore, this would allow a direct comparison with the neutral peptide spectrum in Figure 3. Unfortunately, the FEL used for the IRMPD experiments cannot access this spectral region, and the use of other IR laser sources (e.g., OPO/OPA systems) in combination with the FTICR mass spectrometer is not available to us at this time.

Discussion

It is first necessary to discuss the "quality of fit" obtained by comparing the theoretical to experimental results. Due to the different nature of the neutral and protonated peptide experiments, we discuss each comparison individually. A careful inspection of Figure 3 strongly suggests assignment of **N2** as the dominant neutral Ac-VQIVYK-NHMe conformer. Using the vibrational spectra alone, this assignment is only a suggestion. The **N4** spectrum matches almost as well, and it could be suggested that **N1** is present in some minor population. However, the relative energies in Table 1 provide independent evidence for the favored peptide conformations. While **N2** is not the predicted global minimum, it does fall within the expected level of accuracy, and as noted above, it is possible that **N1** is present as a minor species. **N3** is predicted to be energetically favorable at the M05-2X/6-311++G(d,p) level, but its predicted spectrum clearly does not agree with the experiment. **N4** could agree with the experiment, but it is much higher in energy. The neglect of dispersion energy in the B3LYP functional could conceivably cause errors due to the Tyr side chain, but this deficiency is at least partially addressed by using the M05-2X functional for single-point energies. We emphasize that at least on this point the experiments provide a clear answer: the Tyr must be free on the basis of the OH stretch band observed at 3655 cm^{-1}, essentially unshifted from the gas-phase amino acid.[49] When considered together, the IR spectra and computed energies provide strong evidence for the present conformational assignment.

In the protonated peptide, a close inspection of Figure 5, especially Figure 5B, suggests **P1** as the best-fit conformer on the basis of rather subtle differences in the amide I/II bands. However, **P2** and **P4** could also fit the IRMPD spectrum to some extent. Notably, all three of these conformers are quite similar in that they present interactions between the Lys NH_3^+ and three carbonyl groups (**P3** only has two such interactions). Turning to the energies in Table 2, **P1** is most favorable based on free energies, but both **P2** and **P4** are reasonable, depending on the DFT functional used. Under the 298 K experimental conditions here, the idea of a single specific conformation is probably not realistic. With the IR spectra and energies taken together, **P1** is most likely representative of the dominant average conformation,

(55) Gregoire, G.; Gaigeot, M. P.; Marinica, D. C.; Lemaire, J.; Schermann, J. P.; Desfrancois, C. *Phys. Chem. Chem. Phys.* **2007**, *9*, 3082–3097.

with moderate and large-amplitude motion leading to interconversion between **P2** and **P4** (and perhaps even **P3**) occurring on the experiment time scale.

The ^{306}VQIVYK^{311} sequence in the tau peptide is a "nucleating sequence"[11] and is essential for tau amyloid fibril formation.[10,12] In the amyloid fibrils, the VQIVYK peptide backbone is extended in a β-sheet conformation, enabling fibril formation via cross-β-sheet steric zippers.[13] The results presented here yield valuable insight into the inherent conformation(s) of the gas-phase Ac-VQIVYK-NHMe peptide and allow for comparison and contrast to the crystal structure. By combining IR/UV double-resonance spectroscopy in a cold molecular beam with DFT calculations, we have shown that in the absence of water or other peptides (as would be found in the biological medium of the native-state or amyloid-fibril state tau protein) the neutral Ac-VQIVYK-NHMe peptide adopts a folded β-hairpin-like structure represented best by conformer **N2** (see Figures 2 and 3). Indeed, the other plausible conformer, **N4**, has a very similar β-turn conformation. In the computed **N2** and **N4** structures, the interstrand NH→O═C hydrogen bonds are not as well-formed as in other β-hairpin or β-sheet peptides, for example, gramicidin S,[51] although due to the relatively low resolution in the IR spectrum (Figure 3), this prediction cannot be quantitatively verified here.

Clearly, the folded gas-phase conformation is not the same as the extended β-strand structure observed in amyloid fibrils. However, there are important similarities. The two halves of the β-turn structure are indeed extended, similar to β-strands (note that they are not true β-strands because the ϕ, Ψ angles do not all fall into the upper left quadrant of the Ramachandran diagram). It is notable that all four computed conformers (Figure 2) exhibit this extended motif, even though it appears **N2** is dominant. Furthermore, in **N2** the amino acid side chains do not appear to interfere too much with the backbone conformation (see Figure 2B). Finally, from both the experimental and theoretical NH stretch spectra, the NH→O═C hydrogen bonding between the two backbone halves appears relatively weak, based on the relationship between the hydrogen-bonded NH stretch frequency and the hydrogen-bond strength. These observations are consistent with the hypothesis that the VQIVYK sequence naturally prefers more open and extended backbone conformations, which are more amenable to β-sheet and, ultimately, amyloid fibril formation.

We have also shown that conformational information regarding the protonated form of the isolated peptide sequence can be obtained by combining IRMPD spectroscopy in a (298 K) FTICR mass spectrometer with DFT calculations (Figures 4 and 5). Conformational changes upon protonation can be readily characterized by contrasting the **N2** conformer with the "best-fit" dominant Ac-VQIVYK(H^+)-NHMe conformer, **P1**. Protonation at the Lys side chain significantly alters the isolated Ac-VQIVYK-NHMe backbone conformation as the Lys NH_3^+ binds to three peptide C═O groups and induces a transition between the β-hairpin-like **N2** structure and a coiled, almost helical, **P1** conformation. Note that this conclusion could also be drawn for the other low-energy conformers, especially **P4**, which is very similar to **P1** and energetically favorable with the M05-2X calculations. Thus, the results presented here strongly suggest that protonation disrupts the inherent preference of the VQIVYK sequence for an extended peptide backbone. Indeed, a dramatic conformational change upon Lys protonation is a reasonable outcome in a gas-phase peptide, in which the Lys NH_3^+ is not solvated by water molecules or other molecules. The NH_3^+→*O*═C interaction energy is estimated at ~80−100 kJmol,[56] which is clearly larger than the energetic differences in Table 1. Energy differences between β-hairpin and coiled backbone conformations in the neutral peptide are not likely more than 80 kJ/mol. Thus, the energetic cost of distorting the β-hairpin in the neutral peptide is easily compensated by the strong NH_3^+−backbone interaction.

The conformational change between neutral and protonated Ac-VQIVYK-NHMe is also in a sense consistent with the real-world tau amyloid fibers, where the protonated NH_3^+ from the lysine side chain faces the inner or outer medium, either bound to a counteranion or buried elsewhere in the protein fibril.[57] Our results suggest that preventing the protonated Lys from interacting with the peptide backbone is an essential element for steric zipper and, ultimately, amyloid formation.

Conclusions

We have investigated the inherent conformational preferences of the isolated amyloidogenic tau peptide sequence ^{306}VQIVYK^{311}, a known key element for the tau protein fibril formation. The neutral capped hexapeptide Ac-VQIVYK-NHMe was characterized in a cold molecular beam using IR/UV double-resonance spectroscopy. To characterize the effect of ionic charge on the backbone conformation, the protonated peptide ion, Ac-VQIVYK(H^+)-NHMe, was isolated in a 298 K FTICR mass spectrometer and studied using IRMPD spectroscopy in the fingerprint and amide I/II band region. The conformations for both neutral and protonated species were predicted from an extensive conformational search procedure combined with cluster analysis and followed by DFT calculations.

Comparison between the experimental and computed IR spectra provides evidence for the dominant, preferred conformations of the neutral and protonated peptides. The relative energies and, for the protonated peptide, relative free energies, provide further independent guidelines. Taken together, the two pieces of evidence show that the neutral Ac-VQIVYK-NHMe adopts a β-hairpin-like structure with a β-turn in the middle and two extended β-strand-like peptide halves. The cationic Ac-VQIVYK(H^+)-NHMe adopts a coiled conformation where the Lys NH_3^+ binds to backbone C═O groups and completely disrupts the neutral extended conformation. Thus, the neutral peptide sequence does exhibit preference for extended peptide backbone segments, even though it cannot adopt the full β-strand conformation observed in amyloid fibrils. This preference for extended structures is destroyed by Lys protonation, indicating that tying up the charged Lys side chain NH_3^+ in the amyloid fibril is essential for the fibril and steric zipper formation. These results provide valuable insight into the preferred conformations of a known amyloidogenic peptide sequence and pave the way for future gas-phase studies of Ac-VQIVYK-NHMe peptide aggregates. Such investigations are currently under way in our laboratory.

Acknowledgment. The authors would like to thank Prof. John P. Simons for valuable insight and helpful discussions, and Dr. Louise C. Serpell for helpful comments on the manuscript. The authors gratefully acknowledge the support by the Stichting voor Fundamenteel Onderzoek der Materie (FOM) in providing the required beam time on FELIX and highly appreciate the skillful

(56) Wu, J.; Gard, E.; Bregar, J.; Green, M. K.; Lebrilla, C. B. *J. Am. Chem. Soc.* **1995**, *117*, 9900–9905.
(57) Inouye, H.; Sharma, D.; Goux, W. J.; Kirschner, D. A. *Biophys. J.* **2006**, *90*, 1774–1789.

assistance of the FELIX staff. The authors also gratefully acknowledge the use of the Oxford Supercomputing Centre facilities for this work. The authors are grateful for the support provided by the Royal Society USA/Canada Research Fellowship (T.D.V.) and University Research Fellowship (L.C.S.); the Leverhulme Trust (Grant F/08788G); Corpus Christi College, Oxford (S.G., T.D.B., L.C.S.); and Linacre College, Oxford (T.D.V.).

Supporting Information Available: Full citation for ref 46, Figures S1 and S2, and Cartesian coordinates for conformers **N1**−**N4** and **P1**−**P4**. This information is available free of charge via the Internet at http://pubs.acs.org.

JA804213S